

**Electronic Supplementary Information (ESI)
for**

**Quad-Metallic MOF-Derived Carbon-Armored Pseudo High
Entropy Alloy as Bifunctional Electrocatalyst for Alkaline Water
Electrolysis at High Current Densities**

**Duraisamy Senthil Raja, Yu-Chieh Ting, Ting-Yu Lin, Chih-Chieh Cheng, Po-Wei Chen,
Fan-Yu Yen, Shih-Yuan Lu***

Department of Chemical Engineering, National Tsing Hua University, Hsinchu 300044, Taiwan.

*Email: sylu@mx.nthu.edu.tw (S.-Y. Lu)

General experimental details

Chemicals

Iron(II) chloride tetrahydrate ($\text{FeCl}_2 \cdot 4\text{H}_2\text{O}$, ≥99%, Sigma-Aldrich), cobalt(II) nitrate hexahydrate ($\text{Co}(\text{NO}_3)_2 \cdot 6\text{H}_2\text{O}$, ≥98%, Sigma-Aldrich), nickel (II) nitrate hexahydrate ($\text{Ni}(\text{NO}_3)_2 \cdot 6\text{H}_2\text{O}$, ≥98%, Sigma-Aldrich), molybdenum(V) chloride (MoCl_5 , 95%, Sigma-Aldrich), 2,5-dihydroxyterephthalic acid (DHTA, 98%, Sigma-Aldrich), N,N-dimethylformamide (DMF, anhydrous, 99.8%, Sigma-Aldrich), ethanol (>99%, ECHO Chemical), potassium hydroxide (KOH, 50% w/v, Showa), nickel foam (NF, thickness: 1.7 mm, May Chun Co., Ltd), graphite rods (Alfa Aesar), and Pt wire (CH Instruments) were used as received without further purification. Deionized water (resistivity: 18.2 $\text{M}\Omega \cdot \text{cm}$) was used for preparation of all aqueous solutions. Nickel foam was cut into $3 \times 3 \text{ cm}^2$ pieces, cleaned with ultrasonication in a 3 M HCl solution for 30 min, washed alternately with acetone and water three times, and dried in an oven at 60 °C for 2 h for later use.

Characterizations

Morphologies of the samples were characterized with a field emission scanning electron microscope (FE-SEM, Hitachi S-4800). High-angle annular dark-field scanning transmission electron microscopy (HAADFSTEM) and STEM-mode energy dispersive X-ray spectroscopy (STEM-EDS) were conducted using an aberration-corrected transmission electron microscope (TEM, JEM-ARM200FTH) to characterize the crystalline structure of the samples. Powder XRD patterns of synthesized MOFs and MOF-derived alloy samples (scratched off from NF) were recorded on an X-ray diffractometer (D8 ADVANCE Eco) with $\text{Cu K}\alpha$ as the light source. Metallic elements of the samples were quantified with inductively coupled plasma with optical emission spectrometry (ICP-OES, iCAP 7000 series, Thermo Fisher Scientific). Nitrogen gas adsorption and desorption isotherms (ASAP 2010, Micromeritics Inc., Norcross, GA) were measured at 77 K

for all MOF-derived samples scratched off from NF. Specific surface areas of the MOF-derived products were determined based on the Brunauer-Emmett-Teller (BET) model. Surface chemical states of constituent elements of the samples were investigated using a high resolution X-ray photoelectron spectrometer (HR-XPS, PHI Quantera SXM). Raman spectra of the samples were recorded on a Raman spectrometer (MRID, ProTrusTech Co., Ltd) using a green laser of an excitation wavelength of 532 nm as the light source. Hydrogen and oxygen gases produced during the overall water splitting process for Faradaic efficiency determination were examined with a gas chromatography (GC-2014, SHIMADZU) instrument equipped with a thermal conductivity detector.

Electrochemical measurements

All electrochemical characterizations were conducted on a CHI workstation (CHI Instruments, CHI 6275D) at room temperature in a three-electrode set-up. An Hg/HgO (1 M NaOH) electrode was used as the reference electrode. The electrode potential of Hg/HgO [0.107 vs. normal hydrogen electrode (NHE)] was calibrated according to a recently reported method.¹ Graphite rod for HER and platinum wire for OER were used as the counter electrodes with the NF based samples serving as the working electrodes. Linear sweep voltammetry (LSV) polarization curves were recorded at a scan rate of 1 mV s⁻¹. Potentials reported were converted to refer to reversible hydrogen electrode (RHE) and iR-compensated. Prior to measurements, the working electrode was conditioned with 30 cyclic voltammetry (CV) cycles at a scan rate of 100 mV s⁻¹ to stabilize the current density. Chronopotentiometry (V-t) stability test was conducted at a current density of 500 mA cm⁻² for more than 50 hours for OER, HER, and overall water splitting in 1 M KOH solution. Electrochemical impedance spectroscopy (EIS) spectra were recorded at a specific potential, under which all sample electrodes undergo HER or OER, within a frequency range of 100 kHz to 1 Hz.

A reported reduction peak method was adopted to quantify the total number of surface active sites present in the sample for turnover frequency (TOF) calculations.² In details, a CV curve is first recorded in 1 M KOH for the catalyst, from which the reduction peak area of the curve can be measured. The area is divided by the scan rate to give the total charge of the reduction process, from which the number of electrons actively involved in the reduction process can be calculated by dividing the total charge by the unit charge of an electron (1.602×10^{-19} C). Here, the reduction process is considered as a single electron transfer reaction, and hence, the number of electrons obtained above is exactly the same as the number of surface-active sites (Γ). From the value of Γ , the TOF can be calculated based on the following equation,

$$\text{TOF} = (j \times N_A)/(n \times F \times \Gamma).$$

Here, j is the current density (A cm^{-2}) at a specific potential, N_A is the Avogadro number, n is the number of electrons transferred to evolve the gas molecule (4 for oxygen and 2 for hydrogen), and F is the Faraday constant (96485 C).

Overall water splitting measurements were conducted on a two-electrode set-up in 1 M KOH. The NF based electrode couple, blank NF//blank NF, Pt-C/NF//IrO₂/NF, or FeCoNiMo@C/NF//FeCoNiMo@C/NF, was first conditioned at a scan rate of 100 mV s⁻¹ with a 30 CV cycles. The LSV measurements were then conducted in the potential range of 0–2 V at a slow scan rate of 1 mV s⁻¹. The potentials are iR-compensated. The Faradaic efficiency of FeCoNiMo@C/NF electrode as both anode and cathode for overall water splitting was determined by comparing the number of moles of oxygen and hydrogen produced experimentally and theoretically. And, the amount of hydrogen and oxygen produced experimentally was determined with a water displacement method.³

Calculation details

Calculation details for the four parameters used for judging formation of solid-solution HEAs of an FCC structure are summarized below

(1) Atomic size difference (δ):

$$\delta = 100 \sqrt{\sum_{i=1}^n c_i \left(1 - \frac{r_i}{\bar{r}}\right)},$$

$$\bar{r} = \sum_{i=1}^n c_i r_i$$

where \bar{r} is the average atomic radius, r_i the atomic radius of the i th element, and c_i the atomic concentration of the i th element.

Element	c_i	r_i	$c_i r_i$	$\left(1 - \frac{r_i}{\bar{r}}\right)$	$c_i \left(1 - \frac{r_i}{\bar{r}}\right)$
Fe	0.2321	1.241	0.288036	0.00046965	0.000109
Co	0.2459	1.251	0.307621	0.00019011	4.67E-05
Ni	0.3292	1.246	0.410183	0.00031434	0.000103
Mo	0.1927	1.363	0.26265	0.00555113	0.00107
		\bar{r}	1.26849	$\sum_{i=1}^n c_i \left(1 - \frac{r_i}{\bar{r}}\right)$	0.001329
				$\sqrt{\sum_{i=1}^n c_i \left(1 - \frac{r_i}{\bar{r}}\right)}$	0.036455
				δ	3.645461

(2) Mixing enthalpy (ΔH_{mix}):

$$\Delta H_{\text{mix}} = \sum_{i=1, i \neq j}^n \Omega_{ij} c_i c_j,$$

where $\Omega_{ij}^{ij} = 4\Delta H_{mix}^{ij}$ is the regular solution interaction parameter between the i th and j th elements

and ΔH_{mix}^{ij} is the enthalpy of mixing of binary liquid alloys.

$$\begin{aligned}\Delta H_{mix} &= \Omega_{FeCo} c_{Fe}c_{Co} + \Omega_{FeNi} c_{Fe}c_{Ni} + \Omega_{FeMo} c_{Fe}c_{Mo} + \Omega_{CoNi} c_{Co}c_{Ni} + \Omega_{CoMo} c_{Co}c_{Mo} + \Omega_{NiMo} \\ &c_{Ni}c_{Mo} \\ &= [4(-1) * 0.2321 * 0.2459] + [4(-2) * 0.2321 * 0.3292] + [4(-2) * 0.2321 * 0.1927] + [4(-5) * \\ &0.2459 * 0.3292] + [4(-5) * 0.2459 * 0.1927] + [4(-7) * 0.3292 * 0.1927] = -5.5403 \text{ kJ mol}^{-1}\end{aligned}$$

(3) Mixing entropy (ΔS_{mix}):

$$\Delta S_{mix} = -R \sum_{i=1}^n c_i \ln c_i, \text{ where } R \text{ is the gas constant.}$$

Element	c_i	$\ln c_i$	$c_i \ln c_i$
Fe	0.2321	-1.46059	-0.339
Co	0.2459	-1.40283	-0.34496
Ni	0.3292	-1.11109	-0.36577
Mo	0.1927	-1.64662	-0.3173
		$\sum_{i=1}^n c_i \ln c_i$	-1.36703
		$-R \sum_{i=1}^n c_i \ln c_i$	11.36614

(4) Valence electron concentration (VEC):

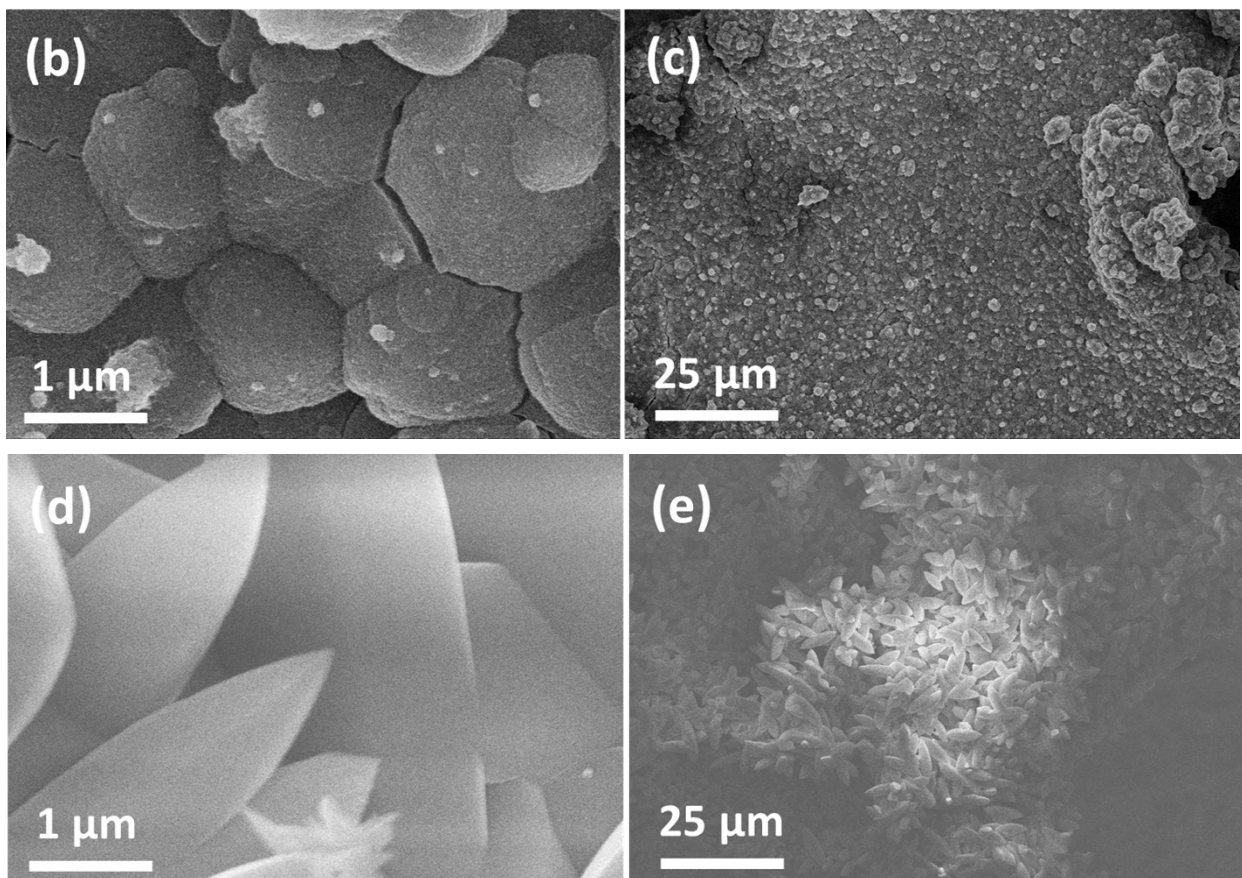
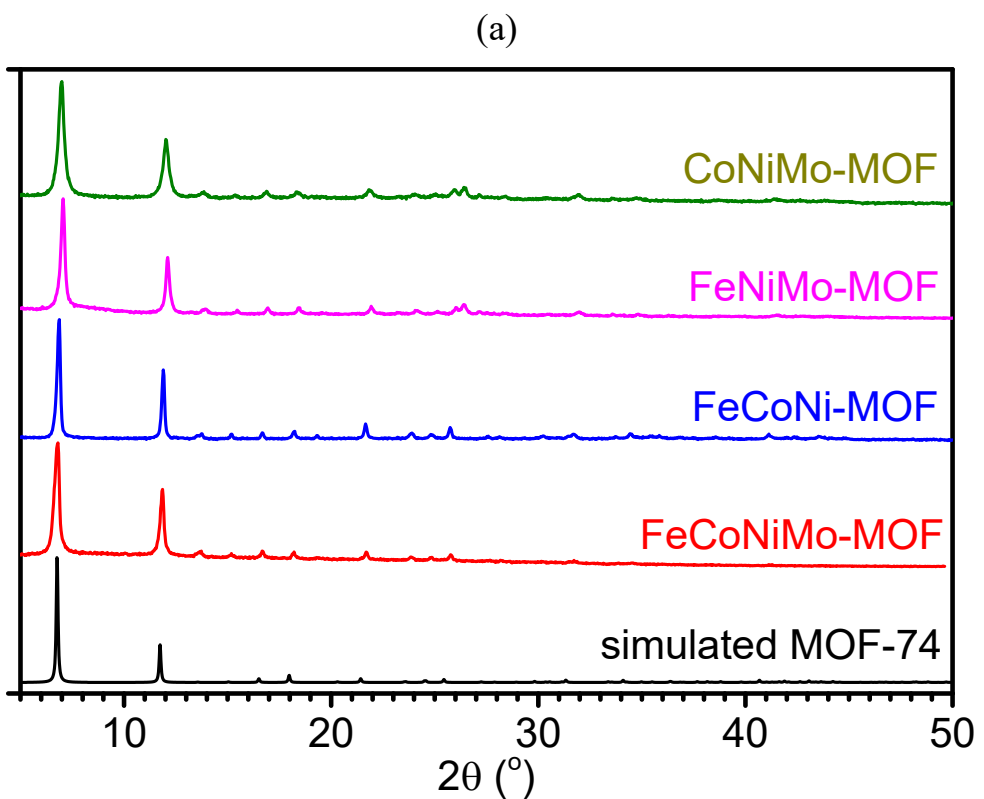
$$VEC = \sum_{i=1}^n c_i (VEC)_i, \text{ where } (VEC)_i \text{ is the VEC for the } i\text{th element.}$$

Element	c_i	$(VEC)_i$	$c_i (VEC)_i$
Fe	0.2321	8	1.8568
Co	0.2459	9	2.2131

Ni	0.3292	10	3.292
Mo	0.1927	6	1.1562
	$\sum_{i=1}^n c_i (\text{VEC})_i$		8.5181

Table S1. Experimental details for syntheses of MOFs on NF.

starting materials	FeCoNiMo-MOF/NF	FeCoNi-MOF/NF	FeNiMo-MOF/NF	CoNiMo-MOF/NF
FeCl ₂ .4H ₂ O (MW: 198.81)	200 mg (1 mmol)	250 mg (1.2 mmol)	360 mg (1.8 mmol)	-
Co(NO ₃) ₂ .6H ₂ O (MW: 291.04)	291 mg (1 mmol)	350 mg (1.2 mmol)	-	524 mg (1.8 mmol)
MoCl ₅ (MW: 273.24)	110 mg 0.4 mmol	-	164 mg (0.6 mmol)	164 mg (0.6 mmol)
H ₂ BDC-(OH) ₂ (MW: 198.13)	240 mg (1.2 mmol)	240 mg (1.2 mmol)	240 mg (1.2 mmol)	240 mg (1.2 mmol)
DMF	35 mL	35 mL	35 mL	35 mL
EtOH	2.5 mL	2.5 mL	2.5 mL	2.5 mL
H ₂ O	2.5 mL	2.5 mL	2.5 mL	2.5 mL
NF substrate	3 cm width & 3 cm height (1.7 mm thickness) placed slantingly			
Reaction condition	150 °C / 48 h (1 h to reach 150 °C, natural Cooling)			
Washing	95% EtOH washing			



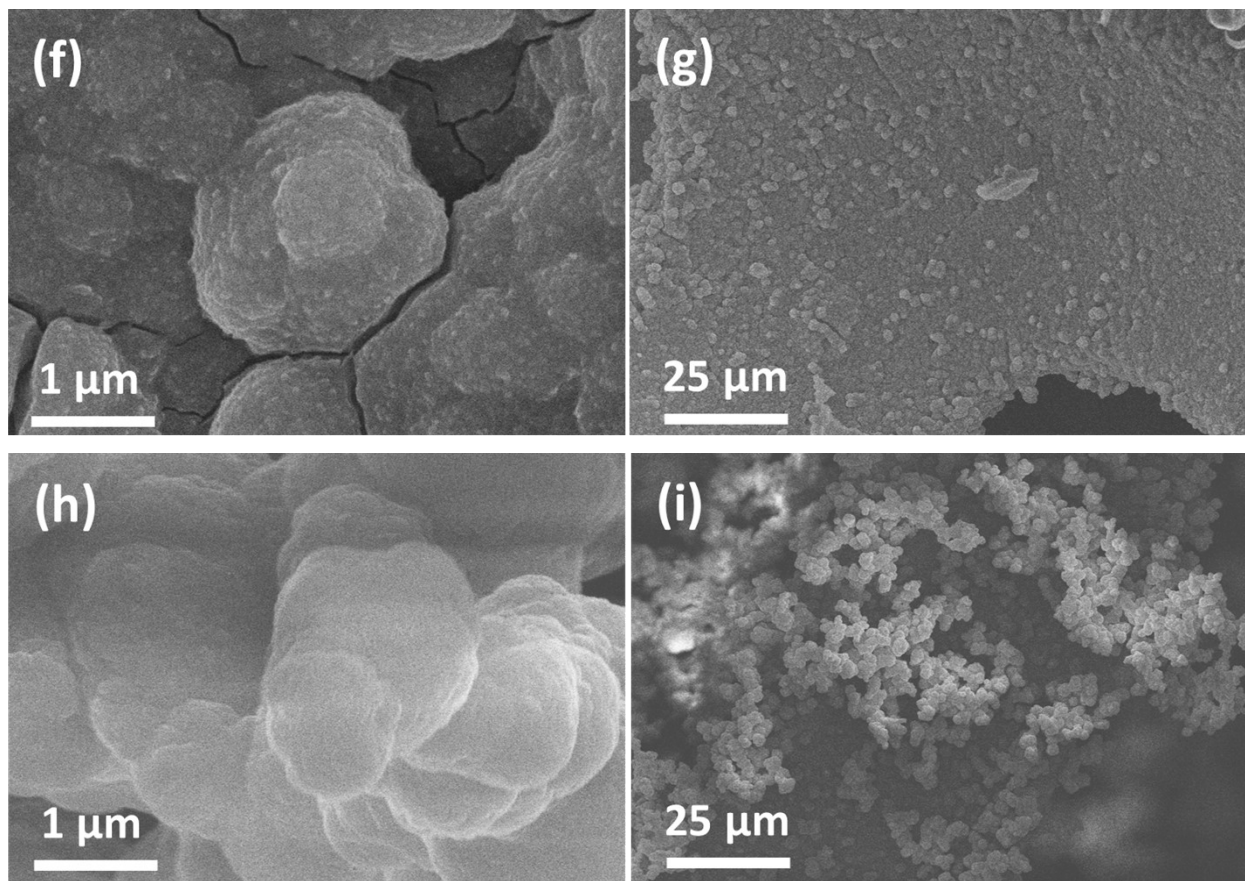
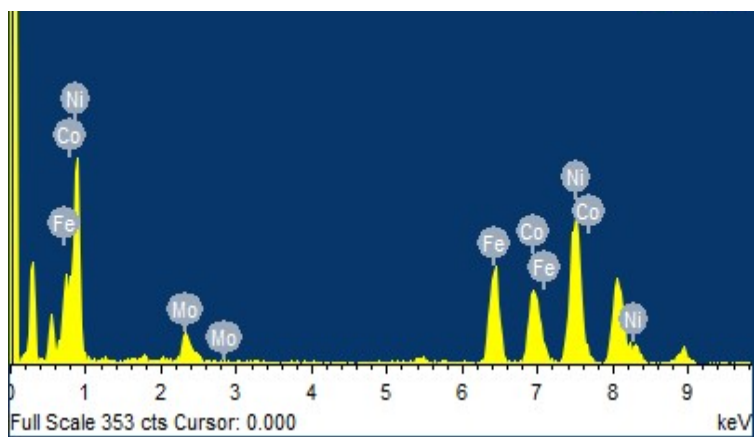
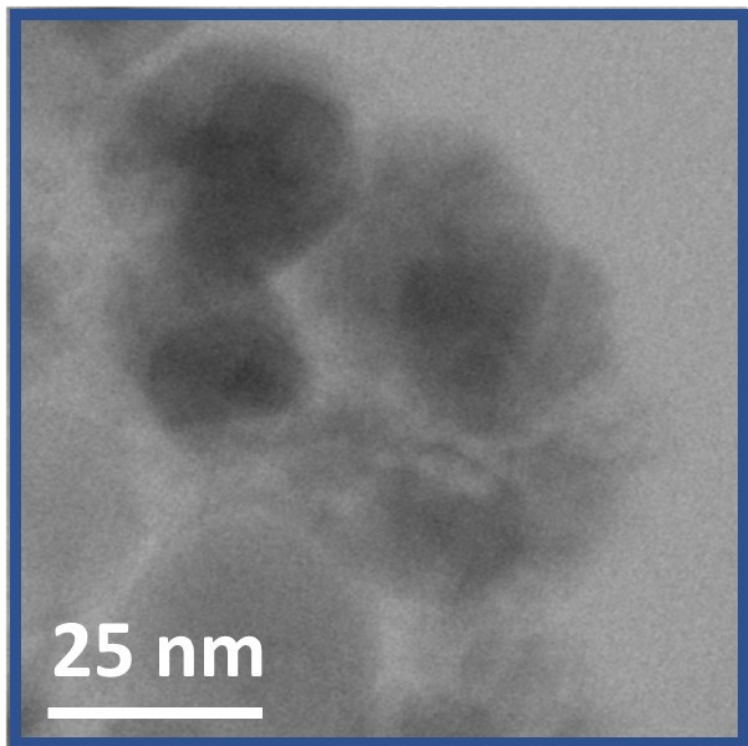


Figure S1. (a) Powder XRD patterns of scratched off MOFs from MOF/NF samples. SEM images of FeCoNiMo-MOF/NF (b, c), FeCoNi-MOF/NF (d, e), FeCoMo-MOF/NF (f, g), and CoNiMo-MOF/NF (h, i).

TEM-EDX Elemental Analysis



Element	Atomic%
Fe K	23.03
Co K	24.12
Ni K	33.64
Mo L	19.21

Figure S2. TEM-EDX elemental analyses of FeCoNiMo@C scratched off from FeCoNiMo@C/NF.

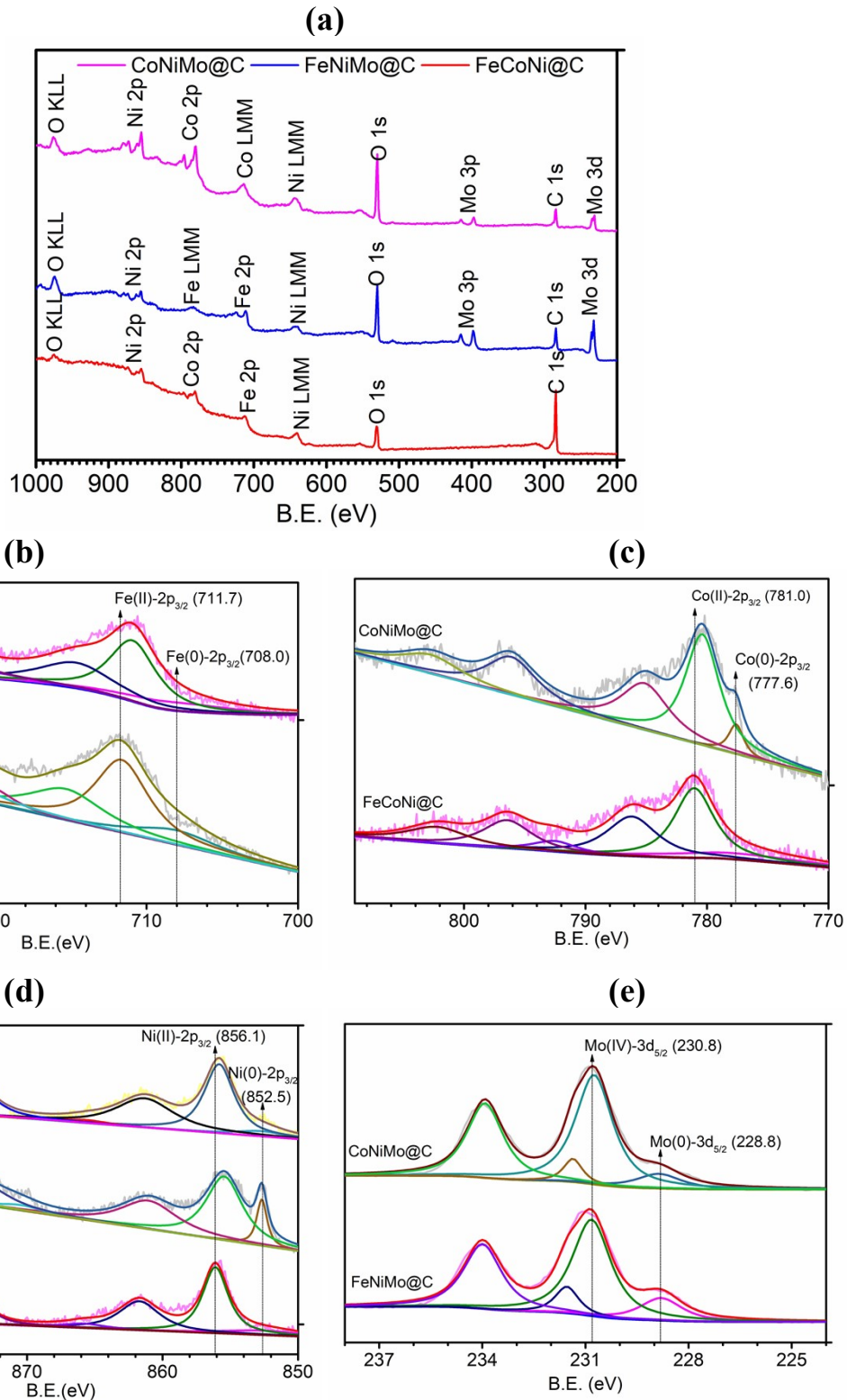


Figure S3. XPS spectra of trimetallic catalysts. (a) Full survey of FeCoNi@C, FeNiMo@C, and CoNiMo@C. (b) HR-XPS of Fe-2p of FeCoNi@C and FeNiMo@C. (c) HR-XPS of Co-2p of FeCoNi@C and CoNiMo@C. (d) HR-XPS of Ni-2p of FeCoNi@C, FeNiMo@C, and CoNiMo@C. (e) HR-XPS of Mo-3d of FeNiMo@C and CoNiMo@C.

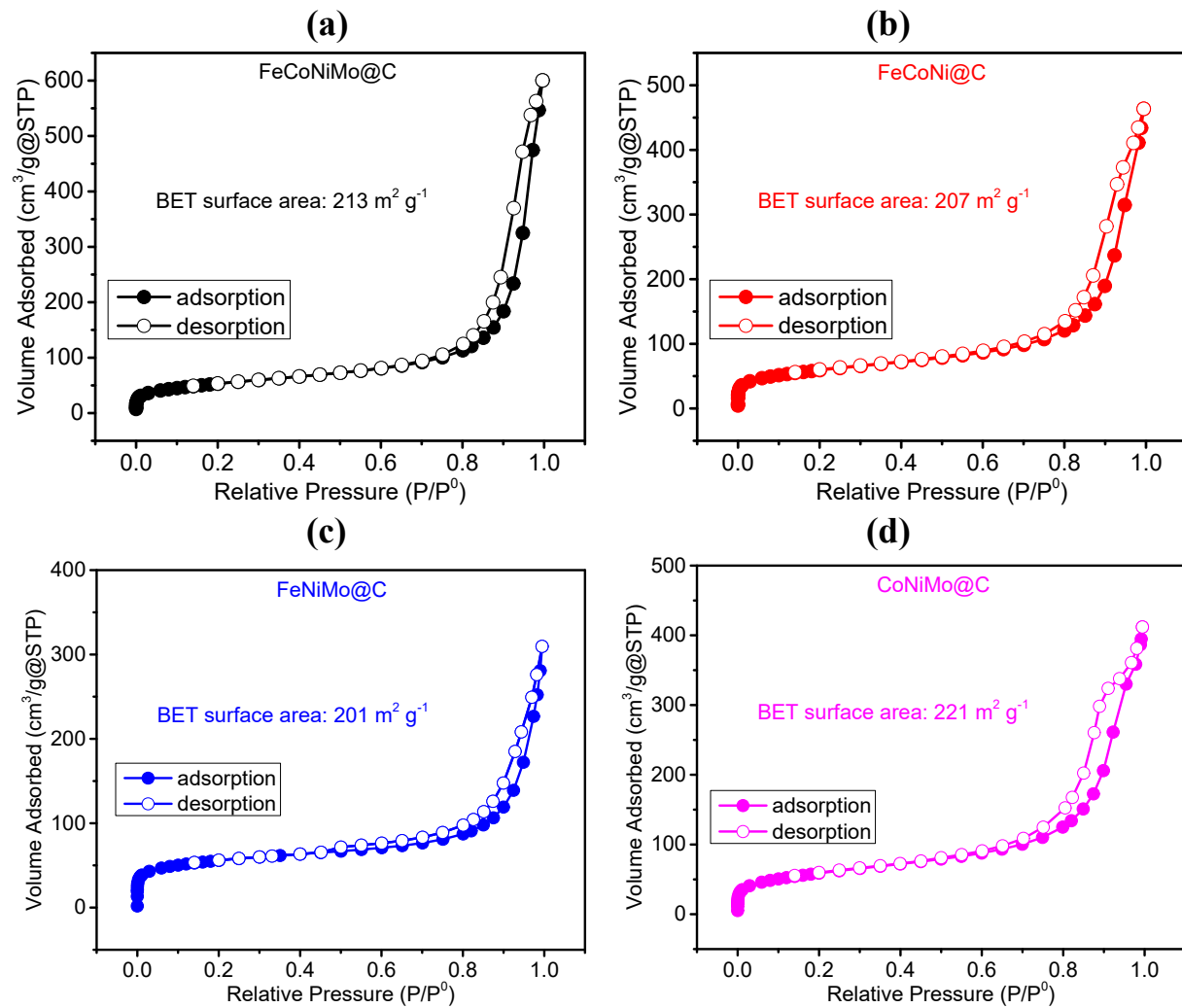


Figure S4. N_2 adsorption/desorption isotherms of (a) FeCoNiMo@C, (b) FeCoNi@C, (c) FeNiMo@C, and (d) CoNiMo@C.

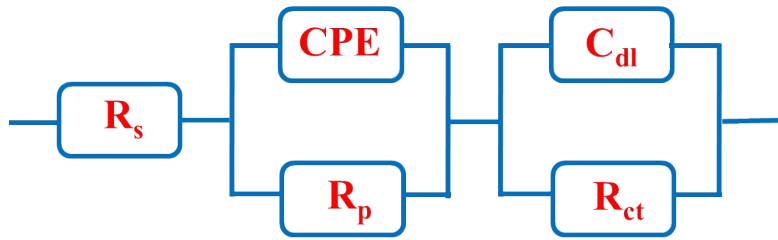


Figure S5. Equivalent circuit model for electrochemical impedance spectroscopy analyses of HER and OER. R_s , R_p , and R_{ct} represent electrolyte, electrode porosity, and charge transfer resistances, respectively, whereas CPE and C_{dl} represent constant phase element and double layer capacitance, respectively.

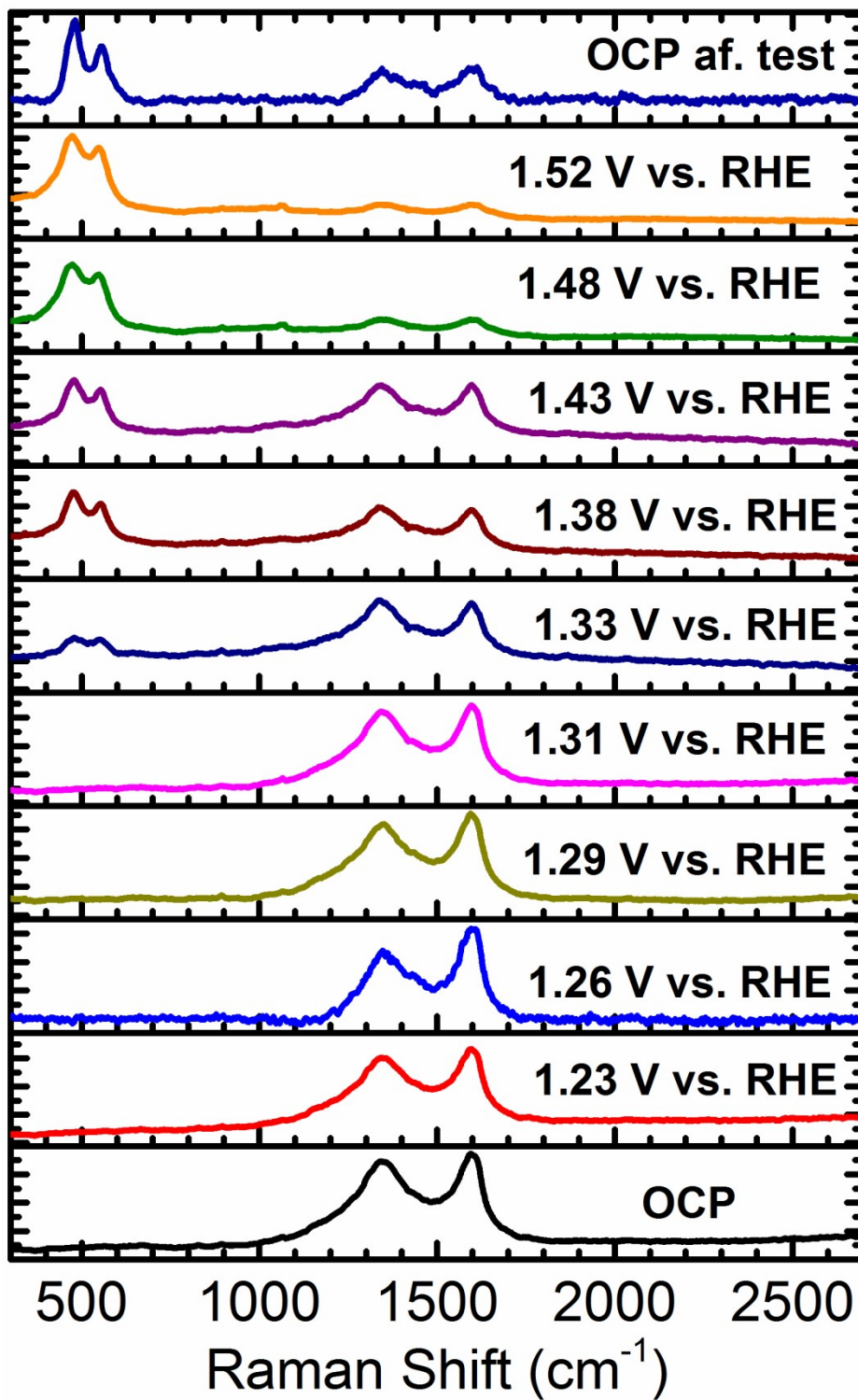


Figure S6. In-situ Raman spectra for FeCoNi@C/NF under citation wavelength of 532 nm and OER conditions at increasing applied potentials (vs. RHE).

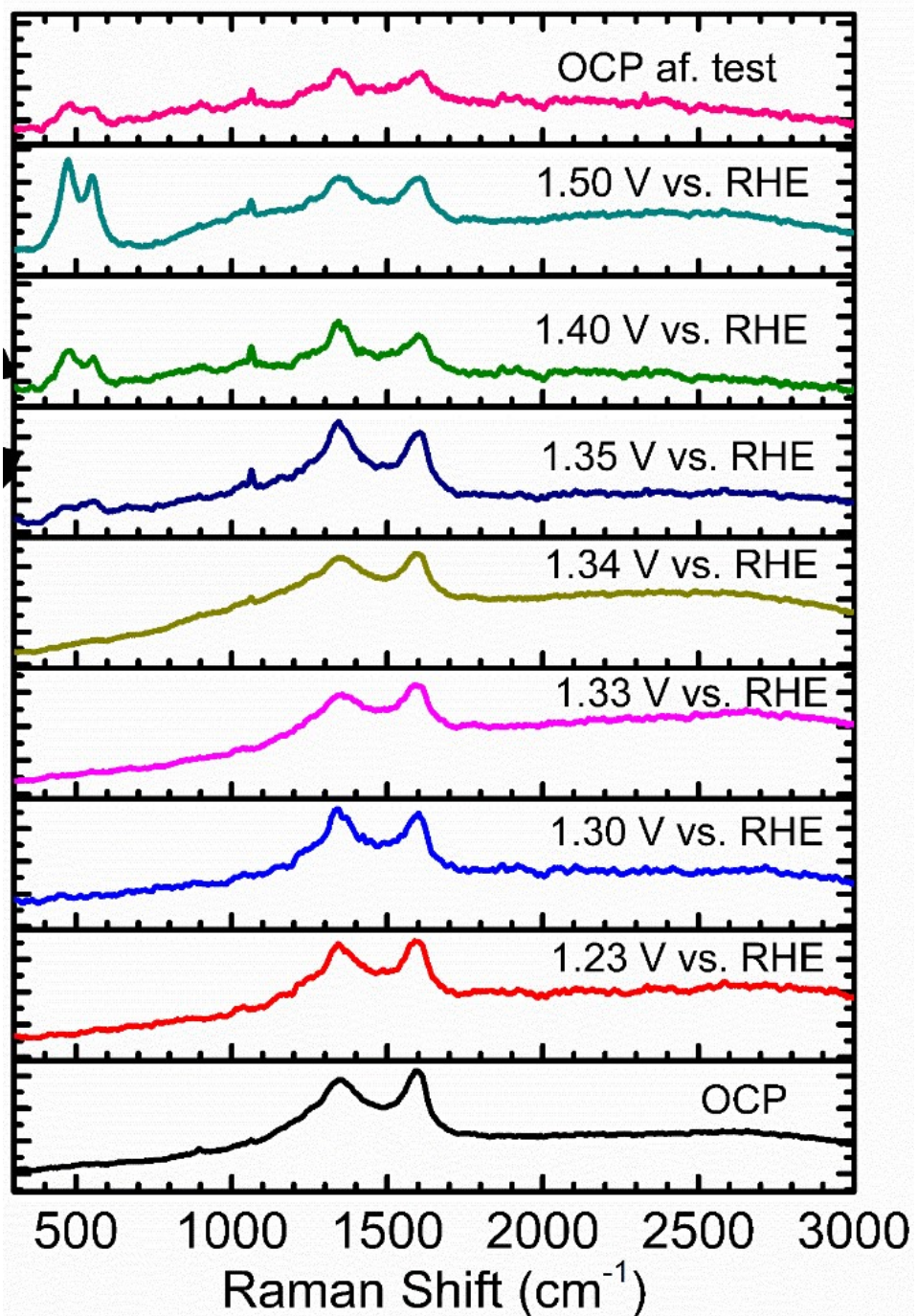


Figure S7. In-situ Raman spectra for FeNiMo@C/NF under citation wavelength of 532 nm and OER conditions at increasing applied potentials (vs. RHE).

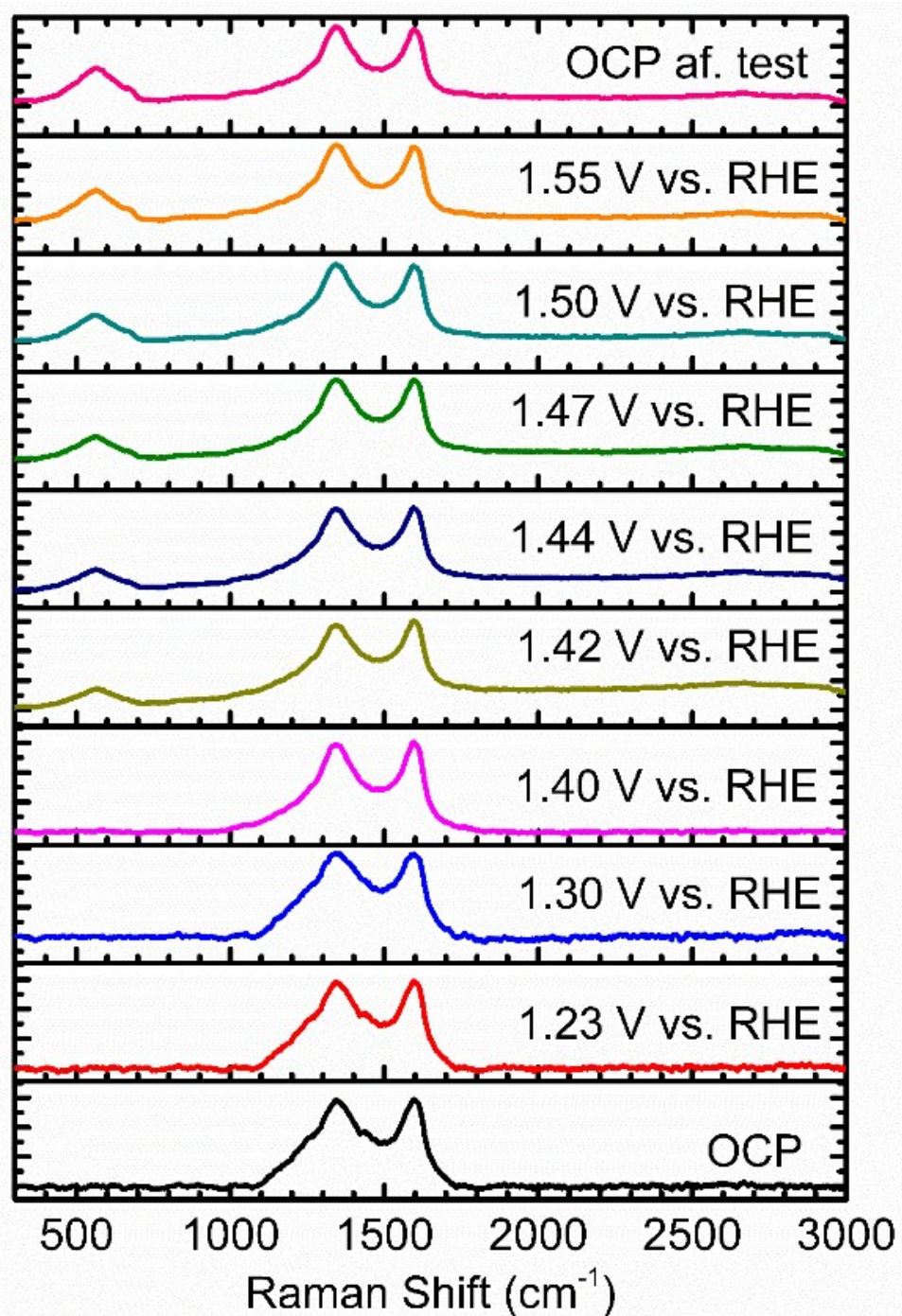


Figure S8. In-situ Raman spectra for CoNiMo@C/NF under citation wavelength of 532 nm and OER conditions at increasing applied potentials (vs. RHE).

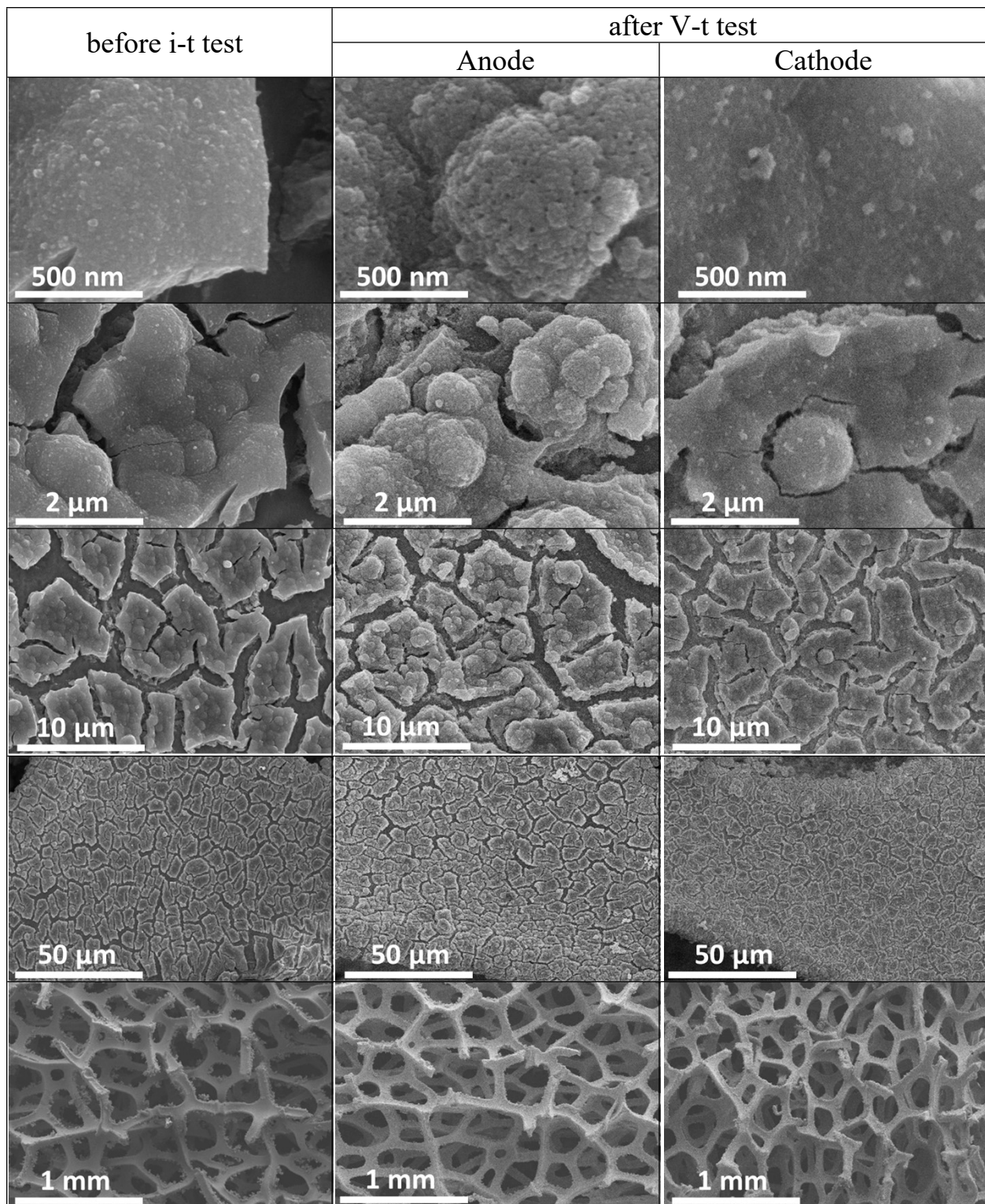


Figure S9. SEM images of FeCoNiMo@C/NF electrode before and after full cell V-t stability test.

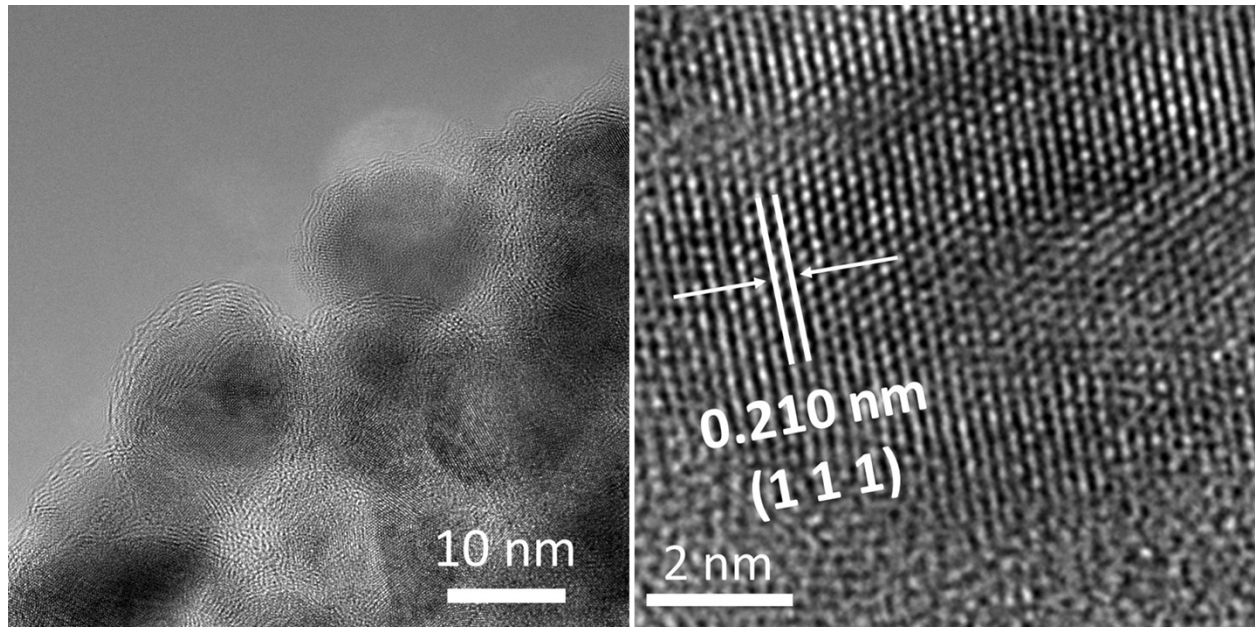


Figure S10. TEM images of FeCoNiMo@C scratched off from FeCoNiMo@C/NF as anode after full cell V-t test for 50 h at 500 mA cm^{-2} .

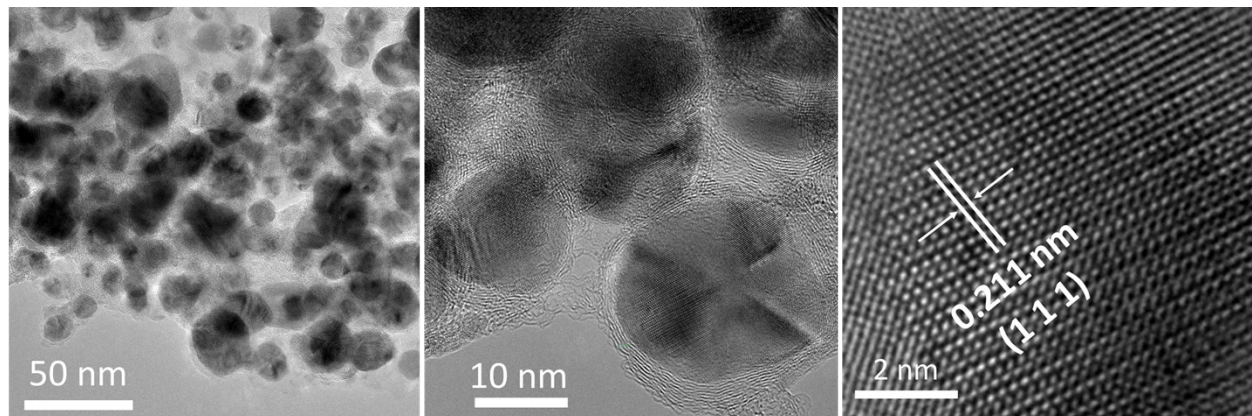


Figure S11. TEM images of FeCoNiMo@C scratched off from FeCoNiMo@C/NF as cathode after full cell V-t test for 50 h at 500 mA cm^{-2} .

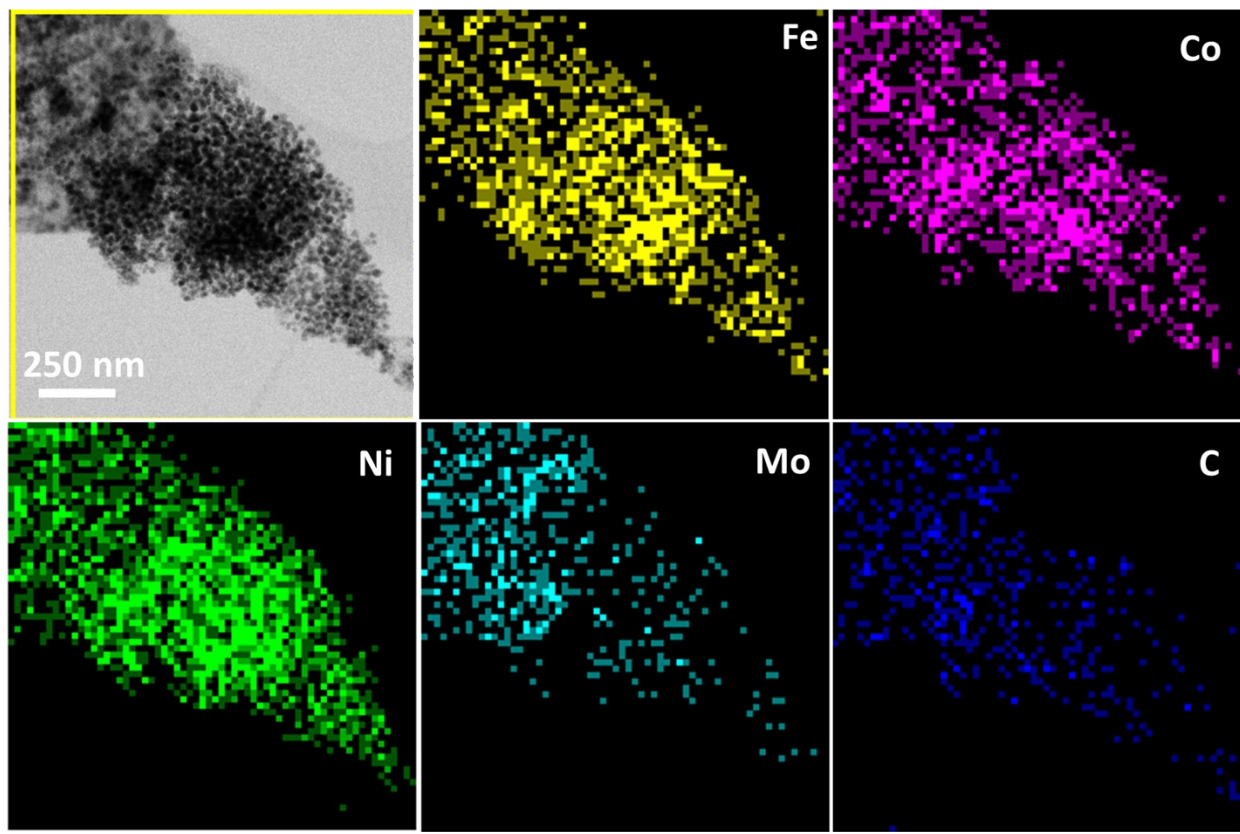


Figure S12. TEM-EDX elemental mapping of FeCoNiMo@C scratched off from FeCoNiMo@C/NF as anode after full cell V-t test for 50 h at 500 mA cm^{-2} .

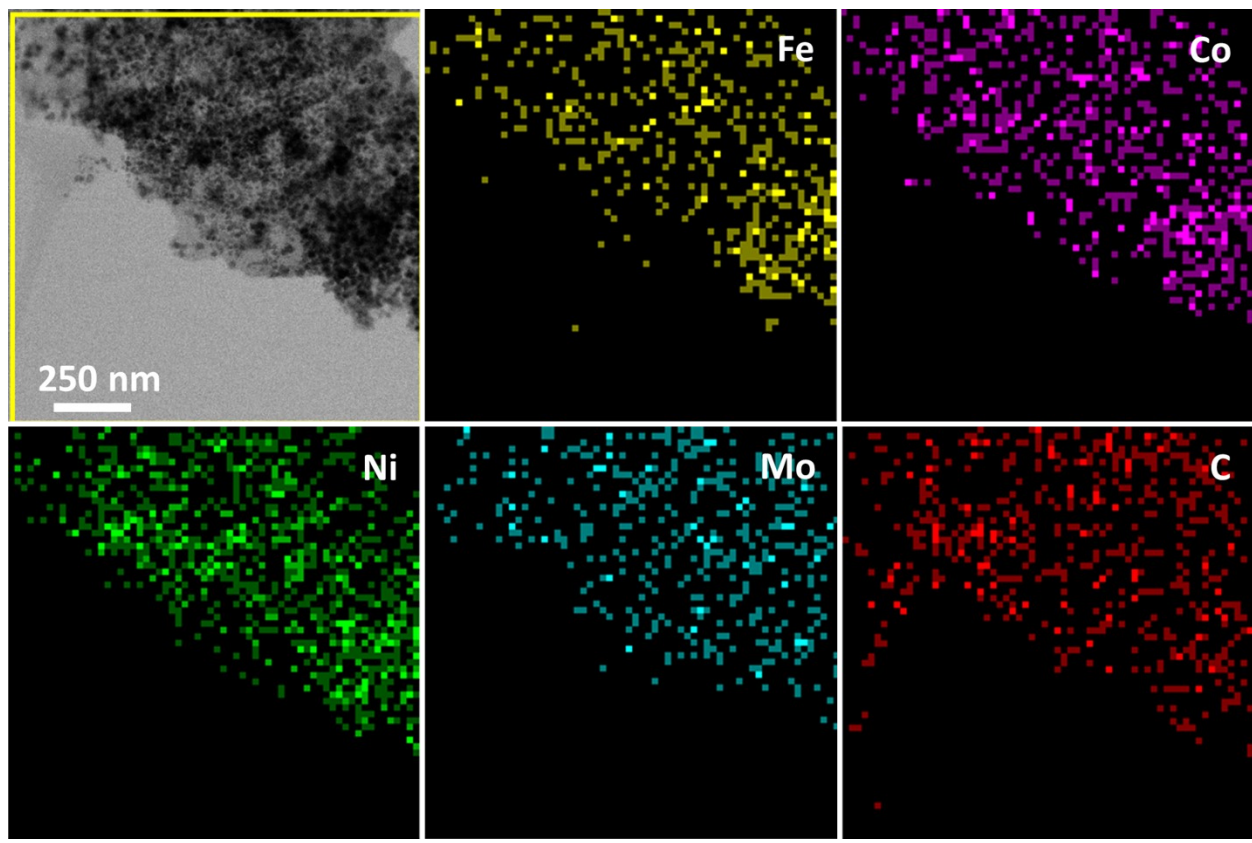


Figure S13. TEM-EDX elemental mapping of FeCoNiMo@C scratched off from FeCoNiMo@C/NF as cathode after full cell V-t test for 50 h at 500 mA cm^{-2} .

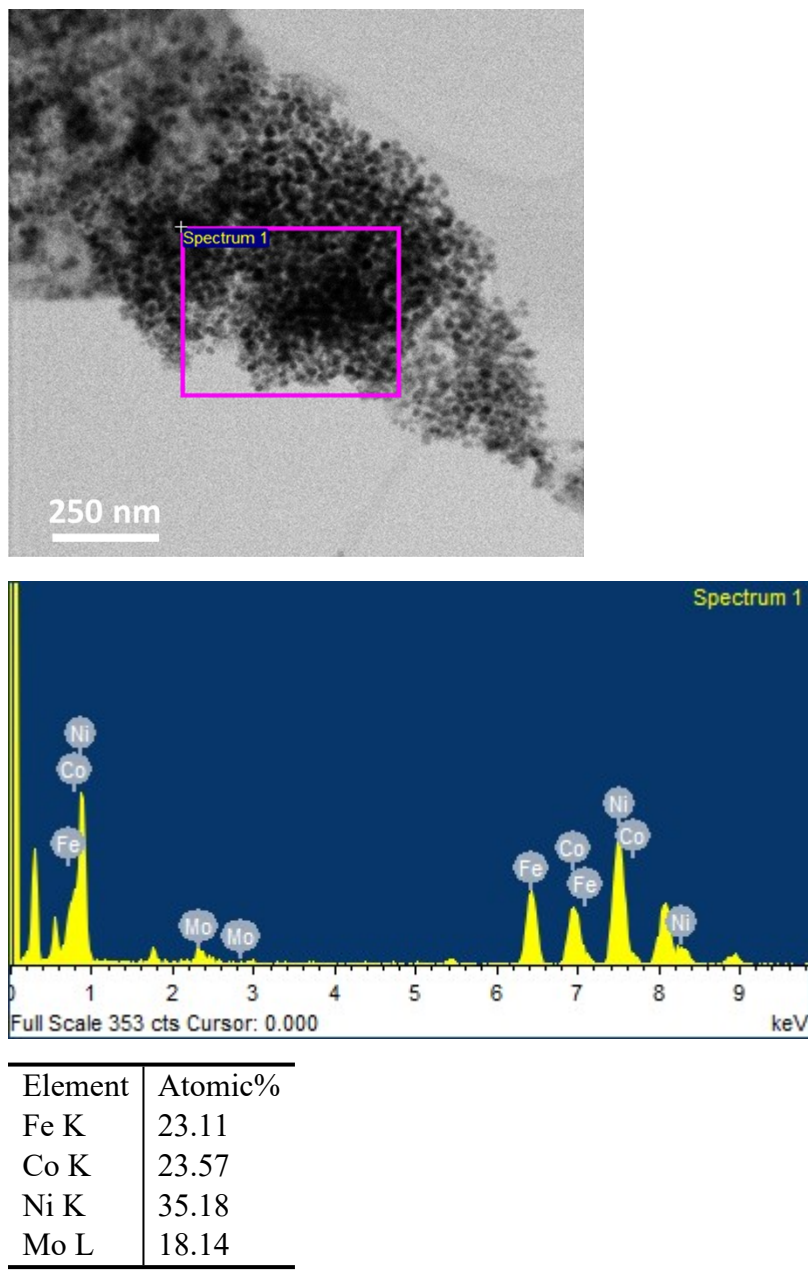
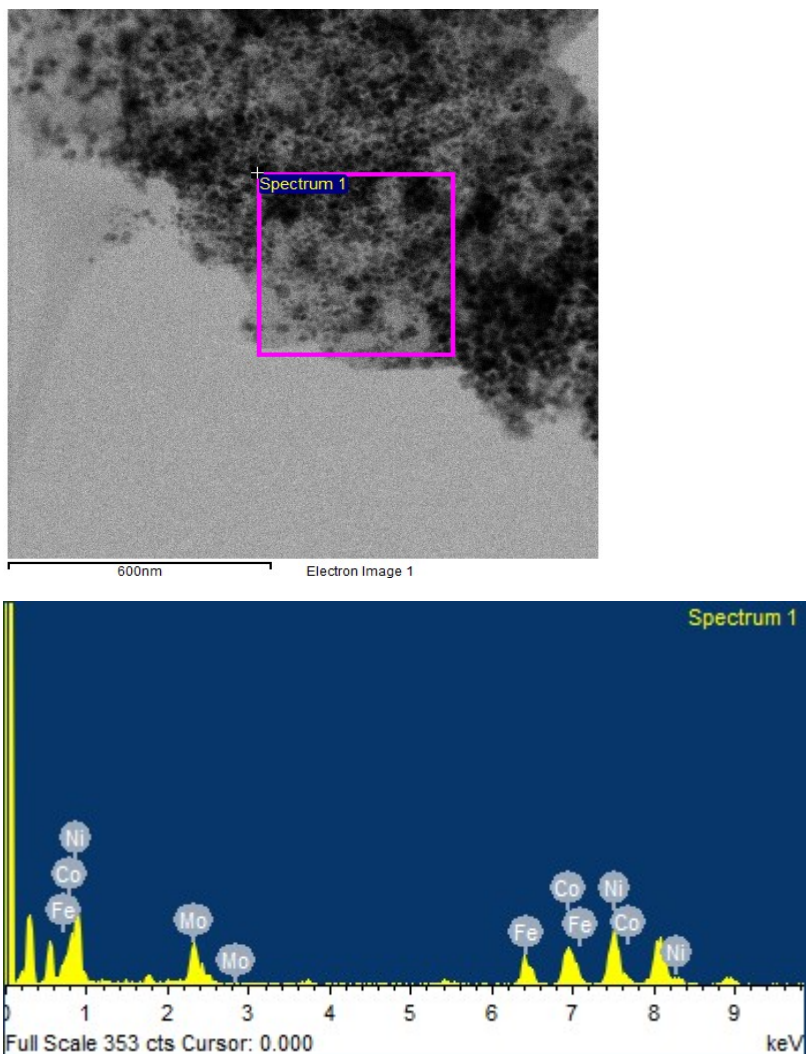


Figure S14. TEM-EDX elemental analysis of FeCoNiMo@C scratched off from FeCoNiMo@C/NF as anode after full cell V-t test for 50 h at 500 mA cm⁻².



Element	Atomic%
Fe K	22.53
Co K	23.71
Ni K	33.94
Mo L	19.82

Figure S15. TEM-EDX elemental analysis of FeCoNiMo@C scratched off from FeCoNiMo@C/NF as cathode after full cell V-t test for 50 h at 500 mA cm^{-2} .

Table S2. ICP-OES results of FeCoNiMo@C scratched off from FeCoNiMo@C/NF before and after full cell V-t stability test. And, ICP-OES results of electrolyte after stability test.

sample	At%
Before V-t test	Fe - 23.21 Co - 24.59 Ni - 32.92 Mo - 19.27
After V-t test Anode	Fe - 22.95 Co - 23.71 Ni - 35.02 Mo - 18.32
After V-t test Cathode	Fe - 22.67 Co - 23.48 Ni - 33.89 Mo - 19.96

ICP-OES results of electrolyte after V-t test

Area of the electrodes used, 0.5 cm²

Loading of FeCoNiCoMo@C on NF = ~0.5 mg cm⁻¹

Loading of FeCoNiCoMo on NF = ~0.45 mg cm⁻¹

Volume of electrolyte = 50 mL

Total weight of electrocatalyst on both electrodes is 0.5 mg (weight of metallic contents ~0.45 mg)

ICP-OES results of electrolyte after V-t test:

Fe = 0.026 ppm

Co = 0.024 ppm

Ni = 0.025 ppm

Mo = 0.040 ppm

Total metallic concentration = 0.115 mg/L

For 50 mL, total weight of metallic content dissolved = 0.00575 mg

% of metallic content dissolved in the electrolyte = (0.00575/0.45)x100 = 1.38%

Table S3. Comparison of electrolytic HER performances of present FeCoNiMo@C with recently reported MOF-derived non-noble metal based HER electrocatalysts in 1 M KOH.

Ref.	Electrocatalyst	η_{10} [mV]	Tafel-slope [mV dec ⁻¹]	Stability
Present work	FeCoNiMo@C/NF	55	56.2	V-t@-500j, 1.8% increase in V @50 h
⁴	CoPS/N C	148	78	-
⁵	MoC _x	151	59	i-t@-15j, ~70% loss in i @11 h
⁶	HC800	123	83	i-t@-30j, no change @2 h
⁷	Co _{0.59} F _{0.41} P	92	76	i-t@-10j, ~30% loss in i @17 h
⁸	Co@BCN	183	73.2	i-t@-17j, no change @10 h
⁹	Ni/C-1	40	77	i-t@-35j, ~20% loss in i @10 h
¹⁰	Co/N-carbon	103	—	i-t@-5j, no change @10 h
¹¹	C-350	47	67	i-t@-10j, no change @40 h
¹²	Co@N-CNTs@rGO	108	55	i-t@-20j, no change @100 h
¹³	Ni@NC-600	250	—	i-t@-10j, ~20% loss in i @12 h
¹⁴	Mo ₂ C/C	165	63.6	i-t@-10j, ~20% loss in i @20 h
¹⁵	nanoMoC@GS(700)	77	50	-
¹⁶	NFP/C-3	95	72	V-t@-10j, no change @12 h
¹⁷	NHPBAP	121	67	V-t@-100j, ~4% increase in V @20 h
¹⁸	Ni/NiO-400	41	59	V-t@-10j, no change @24 h
¹⁹	Ni@NC-rGO	218	99	-
²⁰	CoP/Mo ₂ C-NC	67	66	i-t@-10j, no change @20 h
²¹	Co ₂ Ni ₁ N	102	60	i-t@-10j, no change @24 h
²²	CoNiP nanoboxes	138	65	V-t@-10j, ~40% increase in V @65 h
²³	MoS ₂ /CoS ₂ NTs	85	34	V-t@-10j, no change @72 h

Table S4. Comparison of electrolytic OER performances of present FeCoNiMo@C with recently reported MOF-derived non-noble metal based OER electrocatalysts in 1 M KOH.

Ref.	Electrocatalysts	η_{10} [mV]	Tafel [mV dec ⁻¹]	Stability (j, mA cm ⁻²)
Present work	FeCoNiMo@C/NF	204	33.5	V-t@500j, 2% increase in V @50 h
24	Co ₃ O ₄ /NiCo ₂ O ₄ -DSNCS	340	88	i-t@10j, ~3% loss in i @5 h
25	Co ₃ O ₄ @CoP	238	51.4	V-t@10j, ~1% increase in V @10 h; i-t@250j, ~1% loss in i @24 h
26	NF@NC-CoFe ₂ O ₄ /C NRAS	240	45	V-t@100j, 7.5% increase in V @60 h
27	Co ₃ O ₄ @C-MWCNTs	320	62	V-t@10j, ~0.5% increase in V @25 h
28	Zn doped CoSe ₂ /CFC	356	88	V-t@50j, 1% increase in V @14 h
29	CC@NiCo ₂ O ₄	340	72	i-t@10j, no change @20 h
30	CoTe ₂ @N-GC	300	90	i-t@12j, 25% loss in i @20 h
31	CoO _x -MoC@NC-2	330	89	i-t@7j, no change @10 h
32	CeO _x /CoS	280	50	V-t@10j, ~1% increase in V @20 h
33	CoSe ₂ nanosheet arrays	290	114.7	V-t@10j, ~1% increase in V @24 h
34	NiO/NiCo ₂ O ₄ -rGO	350	66	i-t@10j, no change @5 h
35	Co ₉ S ₈ /NSCNFs-850	302	54	i-t@10j, ~10% loss in i @10 h
36	Ni P nanoplates	300	64	i-t@10j, no change @10 h
37	Fe ₁ Co ₂ -P/C	362	50.1	i-t@4j, ~10% loss in i @8 h
38	Ni Fe-Se cages	240	24	V-t@5j, 0.7% increase in V @22 h
39	CoP@GC	345	56	i-t@10j, no change @10 h
40	HEAN@NPC/CC-450	263	43	i-t@10j, no change @24 h
41	FeCoNiMo HEA/C	250	48	V-t@100j, no change @65 h
42	CoNiCuMnAl@C NF	215	35.6	V-t@200j, no change @30 h
43	Co ₃ O ₄ /C _{BDC}	208	50.1	i-t@65j, ~3% loss in i @36 h
44	Cu@CuO-C-0	340	156	V-t@10j, 2.5% increase in V @10 h
45	NiCo@NiCoO ₂ /C	340	84	V-t@20j, 4.5% increase in V @20 h
46	Co ₃ O ₄ @C-N NSA/NiF	245@25	78	i-t@20j, ~5% loss in i @20 h
47	CoS ₂ @NGC@NF	243	71	i-t@65j, ~6% loss in i @20 h
48	Ni-BDC@NiS	330@20	62	V-t@20j, ~1% increase in V @12 h

Table S5. Comparison of electrolytic water splitting performances of present FeCoNiMo@C with recently reported MOF-derived non-noble metal based bifunctional electrocatalysts in 1 M KOH.

Ref.	Electrocatalysts	HER		OER		Full Cell	
		η_{10} [mV]	Tafel [mV dec ⁻¹]	η_{10} [mV]	Tafel [mV dec ⁻¹]	Voltage [V]@10 mA cm ⁻²	Stability (j, mA cm ⁻²)
Present work	FeCoNiMo@C/NF	55	56.2	204	33.5	1.488	V-t@500j, 3.4% increase in V @50 h
⁴⁹	Co P/NC	154	51	319	52	1.69	i-t@0.8j, no change @24 h
⁵⁰	CoP/rGO-400	150	38	340	66	1.70	-
⁵¹	CoS ₂ NTA/CC	193	88	276	81	1.67	i-t@13j, ~5% loss in i @24 h
⁵²	CoP/NCNHP	115	66	310	70	1.64	V-t@10-100j, no change @36 h
⁵³	CoTe ₂ @NCNTFs	208	58	330	82.8	1.67	i-t@10, no change @30 h
⁵⁴	Co ₃ ZnC/Co-NCCP	188	108	295	70	1.65	i-t@12j, ~5% loss in i @10 h
⁵⁵	Co _{0.2} Fe _{0.8} Ni-OCNF	259	94.2	291	36.1	1.65	V-t@10j, ~3.6% increase in V @24 h
⁵⁶	FeNiP/NCH	216	125	250	68	1.59	V-t@10-100j, no change @40 h
⁵⁷	Co _{0.85} Se@NC	230	125	320	75	1.76	i-t@5-20j, ~5% loss in i @35 h
⁵⁸	Co-NC/CNT	203	125	314	78	1.625	i-t@20j, no change @25 h
⁵⁹	Ni ₃ ZnC _{0.7}	93	48	320	52	1.65	i-t@20j, ~5% loss in i @24 h
⁶⁰	Co4Ni1P	129	52	245	61	1.59	i-t@10j, no change @50 h
⁶¹	Ni@NC-800	205	160	280	45	1.60	i-t@19j, ~5% loss in i @50 h
⁶²	Co _{0.17} Fe _{0.79} P/NC	139	57	299	44	1.66	i-t@40j, no change @35 h
⁶³	FeNi@NC-CNTs	202	113.7	274	45.5	1.80	V-t@10j, no change @11 h
⁶⁴	Ni@CoO@CoNC	190	98	309	53	-	-
⁶⁵	Ni-Fe P@CNRs	74	92.6	217	40	1.52	i-t@20j, no change @24 h
⁶⁶	FeNi ₃ -Fe ₃ O ₄ /MOF-CNT	108	96.8	234	37	1.59	i-t@15j, ~10% loss in i @20 h
⁶⁷	Y-SNi-Co-Se/CFP	250	72	300	87	-	-
⁶⁸	Ni@graphene	240	120	370	66	-	-
⁶⁹	Ni M@C-130	123	50.8	244	47.2	1.565	i-t@10j, 2% loss in i @25 h
⁷⁰	Co ₉ S ₈ -NSC@Mo ₂ C	89	86.7	293	59.7	1.61	i-t@10j, ~12% loss in i @20 h
⁷¹	Co-NCNTFs//NF	141	114	230	94	1.62	i-t@10j, ~10% loss in i @10 h
⁷²	NiCoP NR@NS	71	57	268	71	1.57	i-t@10j, ~20% loss in i @20 h
⁷³	Mo-N/C@MoS ₂	117	64.3	390	72	-	-
⁷⁴	PMo/ZIF-67-6 N	83	50	295	35	1.61	i-t@10j, ~20% loss in i @100 h
⁷⁵	CoNC@MoS ₂ /CNF	143	68	350	51.9	1.62	i-t@21j, ~14% loss in i @28 h
⁷⁶	PNC/Co	298	131	370	76	1.64	-
⁷⁷	Co _{0.6} Fe _{0.4} P-1.125	133	61	298	48	1.57	i-t@25j, 7.5% loss in i @120 h
⁷⁸	Co-NC@Mo ₂ C	99	65	347	61	1.685	i-t@10j, 20.8% loss in i @20 h

⁷⁹	Co-B@CoO/Ti	61	78	190	78	1.56@20	V-t@20j, ~1% increase in V @20 h
⁸⁰	CoP/HNCNP@2D CoP	173	108.7	220	87	1.59	i-t@10j, ~15% loss in i @12 h
⁸¹	Co-Mo ₂ N (S-2-T5)	76	47	302	90	1.576	i-t@11j, ~15% loss in i @44 h
⁸²	Cu _{0.3} Co _{2.7} P/NC	220	122	190	44	1.74	i-t@10j, no change @50 h
⁸³	NF@Ni/C-600	37	57	265	54	1.60@36	i-t@36j, no change @70 h
⁸⁴	ZIF@LDH@NF-600	106	109	318	97	1.59	i-t@11j, ~7.5% loss in i @5 h

References

1. S. Niu, S. Li, Y. Du, X. Han and P. Xu, *ACS Energy Letters*, 2020, **5**, 1083-1087.
2. S. Anantharaj, S. R. Ede, K. Karthick, S. Sam Sankar, K. Sangeetha, P. E. Karthik and S. Kundu, *Energy & Environmental Science*, 2018, **11**, 744-771.
3. E. Detsi, J. B. Cook, B. K. Lesel, C. L. Turner, Y.-L. Liang, S. Robbennolt and S. H. Tolbert, *Energy & Environmental Science*, 2016, **9**, 540-549.
4. Y. Li, S. Niu, D. Rakov, Y. Wang, M. Cabán-Acevedo, S. Zheng, B. Song and P. Xu, *Nanoscale*, 2018, **10**, 7291-7297.
5. H. B. Wu, B. Y. Xia, L. Yu, X.-Y. Yu and X. W. Lou, *Nature Communications*, 2015, **6**, 6512.
6. X. Xu, F. Nosheen and X. Wang, *Chemistry of Materials*, 2016, **28**, 6313-6320.
7. J. Hao, W. Yang, Z. Zhang and J. Tang, *Nanoscale*, 2015, **7**, 11055-11062.
8. H. Zhang, Z. Ma, J. Duan, H. Liu, G. Liu, T. Wang, K. Chang, M. Li, L. Shi, X. Meng, K. Wu and J. Ye, *ACS Nano*, 2016, **10**, 684-694.
9. L. Wang, L. Ren, X. Wang, X. Feng, J. Zhou and B. Wang, *ACS Applied Materials & Interfaces*, 2018, **10**, 4750-4756.
10. T. Huang, Y. Chen and J.-M. Lee, *ACS Sustainable Chemistry & Engineering*, 2017, **5**, 5646-5650.
11. S. Hu, S. Wang, C. Feng, H. Wu, J. Zhang and H. Mei, *ACS Sustainable Chemistry & Engineering*, 2020, **8**, 7414-7422.
12. Z. Chen, R. Wu, Y. Liu, Y. Ha, Y. Guo, D. Sun, M. Liu and F. Fang, *Advanced Materials*, 2018, **30**, 1802011.
13. Z. Huang, J. Liu, Z. Xiao, H. Fu, W. Fan, B. Xu, B. Dong, D. Liu, F. Dai and D. Sun, *Nanoscale*, 2018, **10**, 22758-22765.
14. M. Qamar, A. Adam, B. Merzougui, A. Helal, O. Abdulhamid and M. N. Siddiqui, *Journal of Materials Chemistry A*, 2016, **4**, 16225-16232.
15. Z. Shi, Y. Wang, H. Lin, H. Zhang, M. Shen, S. Xie, Y. Zhang, Q. Gao and Y. Tang, *Journal of Materials Chemistry A*, 2016, **4**, 6006-6013.
16. X. F. Lu, L. Yu and X. W. Lou, *Science Advances*, **5**, eaav6009.
17. Y. Ge, P. Dong, S. R. Craig, P. M. Ajayan, M. Ye and J. Shen, *Advanced Energy Materials*, 2018, **8**, 1800484.

18. Y. Jiao, W. Hong, P. Li, L. Wang and G. Chen, *Applied Catalysis B: Environmental*, 2019, **244**, 732-739.
19. Y. Cao, Y. Lu, E. H. Ang, H. Geng, X. Cao, J. Zheng and H. Gu, *Nanoscale*, 2019, **11**, 15112-15119.
20. X. Luo, Q. Zhou, S. Du, J. Li, L. Zhang, K. Lin, H. Li, B. Chen, T. Wu, D. Chen, M. Chang and Y. Liu, *ACS Applied Materials & Interfaces*, 2018, **10**, 42335-42347.
21. X. Feng, H. Wang, X. Bo and L. Guo, *ACS Applied Materials & Interfaces*, 2019, **11**, 8018-8024.
22. Y. Lu, Y. Deng, S. Lu, Y. Liu, J. Lang, X. Cao and H. Gu, *Nanoscale*, 2019, **11**, 21259-21265.
23. B. Tang, Z. G. Yu, Y. Zhang, C. Tang, H. L. Seng, Z. W. Seh, Y.-W. Zhang, S. J. Pennycook, H. Gong and W. Yang, *Journal of Materials Chemistry A*, 2019, **7**, 13339-13346.
24. H. Hu, B. Guan, B. Xia and X. W. Lou, *Journal of the American Chemical Society*, 2015, **137**, 5590-5595.
25. J. Zhou, Y. Dou, A. Zhou, R.-M. Guo, M.-J. Zhao and J.-R. Li, *Advanced Energy Materials*, 2017, **7**, 1602643.
26. X.-F. Lu, L.-F. Gu, J.-W. Wang, J.-X. Wu, P.-Q. Liao and G.-R. Li, *Advanced Materials*, 2017, **29**, 1604437.
27. X. Li, Y. Fang, X. Lin, M. Tian, X. An, Y. Fu, R. Li, J. Jin and J. Ma, *Journal of Materials Chemistry A*, 2015, **3**, 17392-17402.
28. Q. Dong, Q. Wang, Z. Dai, H. Qiu and X. Dong, *ACS Applied Materials & Interfaces*, 2016, **8**, 26902-26907.
29. C. Guan, X. Liu, W. Ren, X. Li, C. Cheng and J. Wang, *Advanced Energy Materials*, 2017, **7**, 1602391.
30. M. Liu, X. Lu, C. Guo, Z. Wang, Y. Li, Y. Lin, Y. Zhou, S. Wang and J. Zhang, *ACS Applied Materials & Interfaces*, 2017, **9**, 36146-36153.
31. T. Huang, Y. Chen and J.-M. Lee, *Small*, 2017, **13**, 1702753.
32. H. Xu, J. Cao, C. Shan, B. Wang, P. Xi, W. Liu and Y. Tang, *Angewandte Chemie International Edition*, 2018, **57**, 8654-8658.
33. T. Chen, S. Li, J. Wen, P. Gui and G. Fang, *ACS Applied Materials & Interfaces*, 2017, **9**, 35927-35935.

34. Y. Wang, Z. Zhang, X. Liu, F. Ding, P. Zou, X. Wang, Q. Zhao and H. Rao, *ACS Sustainable Chemistry & Engineering*, 2018, **6**, 12511-12521.
35. L.-L. Wu, Q.-S. Wang, J. Li, Y. Long, Y. Liu, S.-Y. Song and H.-J. Zhang, *Small*, 2018, **14**, 1704035.
36. X.-Y. Yu, Y. Feng, B. Guan, X. W. Lou and U. Paik, *Energy & Environmental Science*, 2016, **9**, 1246-1250.
37. W. Hong, M. Kitta and Q. Xu, *Small Methods*, 2018, **2**, 1800214.
38. J. Nai, Y. Lu, L. Yu, X. Wang and X. W. Lou, *Advanced Materials*, 2017, **29**, 1703870.
39. R. Wu, D. P. Wang, K. Zhou, N. Srikanth, J. Wei and Z. Chen, *Journal of Materials Chemistry A*, 2016, **4**, 13742-13745.
40. K. Huang, B. Zhang, J. Wu, T. Zhang, D. Peng, X. Cao, Z. Zhang, Z. Li and Y. Huang, *Journal of Materials Chemistry A*, 2020, **8**, 11938-11947.
41. Y. Mei, Y. Feng, C. Zhang, Y. Zhang, Q. Qi and J. Hu, *ACS Catalysis*, 2022, **12**, 10808-10817.
42. S. Wang, W. Huo, F. Fang, Z. Xie, J. K. Shang and J. Jiang, *Chemical Engineering Journal*, 2022, **429**, 132410.
43. J. Zhou, Y. Dou, A. Zhou, L. Shu, Y. Chen and J.-R. Li, *ACS Energy Letters*, 2018, **3**, 1655-1661.
44. J.-X. Wu, C.-T. He, G.-R. Li and J.-P. Zhang, *Journal of Materials Chemistry A*, 2018, **6**, 19176-19181.
45. H. Xu, Z.-X. Shi, Y.-X. Tong and G.-R. Li, *Advanced Materials*, 2018, **30**, 1705442.
46. X. Kuang, Y. Luo, R. Kuang, Z. Wang, X. Sun, Y. Zhang and Q. Wei, *Carbon*, 2018, **137**, 433-441.
47. L. Pei, J. Zhong, T. Li, W. Bai, S. Wu, Y. Yuan, Y. Chen, Z. Yu, S. Yan and Z. Zou, *Journal of Materials Chemistry A*, 2020, **8**, 6795-6803.
48. P. He, Y. Xie, Y. Dou, J. Zhou, A. Zhou, X. Wei and J.-R. Li, *ACS Applied Materials & Interfaces*, 2019, **11**, 41595-41601.
49. B. You, N. Jiang, M. Sheng, S. Gul, J. Yano and Y. Sun, *Chemistry of Materials*, 2015, **27**, 7636-7642.
50. L. Jiao, Y.-X. Zhou and H.-L. Jiang, *Chemical Science*, 2016, **7**, 1690-1695.
51. C. Guan, X. Liu, A. M. Elshahawy, H. Zhang, H. Wu, S. J. Pennycook and J. Wang, *Nanoscale Horizons*, 2017, **2**, 342-348.

52. Y. Pan, K. Sun, S. Liu, X. Cao, K. Wu, W.-C. Cheong, Z. Chen, Y. Wang, Y. Li, Y. Liu, D. Wang, Q. Peng, C. Chen and Y. Li, *Journal of the American Chemical Society*, 2018, **140**, 2610-2618.
53. X. Wang, X. Huang, W. Gao, Y. Tang, P. Jiang, K. Lan, R. Yang, B. Wang and R. Li, *Journal of Materials Chemistry A*, 2018, **6**, 3684-3691.
54. Z. Yu, Y. Bai, S. Zhang, Y. Liu, N. Zhang, G. Wang, J. Wei, Q. Wu and K. Sun, *ACS Applied Materials & Interfaces*, 2018, **10**, 6245-6252.
55. Y. Li, M. Lu, Y. Wu, H. Xu, J. Gao and J. Yao, *Advanced Materials Interfaces*, 2019, **6**, 1900290.
56. Y.-S. Wei, M. Zhang, M. Kitta, Z. Liu, S. Horike and Q. Xu, *Journal of the American Chemical Society*, 2019, **141**, 7906-7916.
57. T. Meng, J. Qin, S. Wang, D. Zhao, B. Mao and M. Cao, *Journal of Materials Chemistry A*, 2017, **5**, 7001-7014.
58. F. Yang, P. Zhao, X. Hua, W. Luo, G. Cheng, W. Xing and S. Chen, *Journal of Materials Chemistry A*, 2016, **4**, 16057-16063.
59. Y. Wang, W. Wu, Y. Rao, Z. Li, N. Tsubaki and M. Wu, *Journal of Materials Chemistry A*, 2017, **5**, 6170-6177.
60. L. Yan, L. Cao, P. Dai, X. Gu, D. Liu, L. Li, Y. Wang and X. Zhao, *Advanced Functional Materials*, 2017, **27**, 1703455.
61. Y. Xu, W. Tu, B. Zhang, S. Yin, Y. Huang, M. Kraft and R. Xu, *Advanced Materials*, 2017, **29**, 1605957.
62. J. Chen, Y. Zhang, H. Ye, J.-Q. Xie, Y. Li, C. Yan, R. Sun and C.-P. Wong, *ACS Applied Energy Materials*, 2019, **2**, 2734-2742.
63. X. Zhao, P. Pachfule, S. Li, J. R. J. Simke, J. Schmidt and A. Thomas, *Angewandte Chemie International Edition*, 2018, **57**, 8921-8926.
64. G. Cai, W. Zhang, L. Jiao, S.-H. Yu and H.-L. Jiang, *Chem*, 2017, **2**, 791-802.
65. S. H. Ahn and A. Manthiram, *Journal of Materials Chemistry A*, 2017, **5**, 2496-2503.
66. K. Srinivas, Y. Lu, Y. Chen, W. Zhang and D. Yang, *ACS Sustainable Chemistry & Engineering*, 2020, **8**, 3820-3831.
67. K. Ao, J. Dong, C. Fan, D. Wang, Y. Cai, D. Li, F. Huang and Q. Wei, *ACS Sustainable Chemistry & Engineering*, 2018, **6**, 10952-10959.
68. L. Ai, T. Tian and J. Jiang, *ACS Sustainable Chemistry & Engineering*, 2017, **5**, 4771-4777.

69. K. Srinivas, Y. Chen, X. Wang, B. Wang, M. Karpuraranjith, W. Wang, Z. Su, W. Zhang and D. Yang, *ACS Sustainable Chemistry & Engineering*, 2021, **9**, 1920-1931.
70. X. Luo, Q. Zhou, S. Du, J. Li, J. Zhong, X. Deng and Y. Liu, *ACS Applied Materials & Interfaces*, 2018, **10**, 22291-22302.
71. Q. Yuan, Y. Yu, Y. Gong and X. Bi, *ACS Applied Materials & Interfaces*, 2020, **12**, 3592-3602.
72. J.-G. Wang, W. Hua, M. Li, H. Liu, M. Shao and B. Wei, *ACS Applied Materials & Interfaces*, 2018, **10**, 41237-41245.
73. I. S. Amiinu, Z. Pu, X. Liu, K. A. Owusu, H. G. R. Monestel, F. O. Boakye, H. Zhang and S. Mu, *Advanced Functional Materials*, 2017, **27**, 1702300.
74. C. Chen, A. Wu, H. Yan, Y. Xiao, C. Tian and H. Fu, *Chemical Science*, 2018, **9**, 4746-4755.
75. D. Ji, S. Peng, L. Fan, L. Li, X. Qin and S. Ramakrishna, *Journal of Materials Chemistry A*, 2017, **5**, 23898-23908.
76. X. Li, Z. Niu, J. Jiang and L. Ai, *Journal of Materials Chemistry A*, 2016, **4**, 3204-3209.
77. Y. Lian, H. Sun, X. Wang, P. Qi, Q. Mu, Y. Chen, J. Ye, X. Zhao, Z. Deng and Y. Peng, *Chemical Science*, 2019, **10**, 464-474.
78. Q. Liang, H. Jin, Z. Wang, Y. Xiong, S. Yuan, X. Zeng, D. He and S. Mu, *Nano Energy*, 2019, **57**, 746-752.
79. W. Lu, T. Liu, L. Xie, C. Tang, D. Liu, S. Hao, F. Qu, G. Du, Y. Ma, A. M. Asiri and X. Sun, *Small*, 2017, **13**, 1700805.
80. S. Lv, J. Chen, X. Chen, J. Chen and Y. Li, *ChemSusChem*, 2020, **13**, 3495-3503.
81. X. Shi, A. Wu, H. Yan, L. Zhang, C. Tian, L. Wang and H. Fu, *Journal of Materials Chemistry A*, 2018, **6**, 20100-20109.
82. J. Song, C. Zhu, B. Z. Xu, S. Fu, M. H. Engelhard, R. Ye, D. Du, S. P. Beckman and Y. Lin, *Advanced Energy Materials*, 2017, **7**, 1601555.
83. H. Sun, Y. Lian, C. Yang, L. Xiong, P. Qi, Q. Mu, X. Zhao, J. Guo, Z. Deng and Y. Peng, *Energy & Environmental Science*, 2018, **11**, 2363-2371.
84. Y. Tang, X. Fang, X. Zhang, G. Fernandes, Y. Yan, D. Yan, X. Xiang and J. He, *ACS Applied Materials & Interfaces*, 2017, **9**, 36762-36771.